Contents lists available at ScienceDirect

Journal of Environmental Management

journal homepage: www.elsevier.com/locate/jenvman

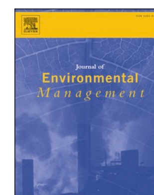

Comparison of UV-A photolytic and UV/TiO_2 photocatalytic effects on *Microcystis aeruginosa* PCC7813 and four microcystin analogues: A pilot scale study

Indira Menezes[a,b,*], José Capelo-Neto[a], Carlos J. Pestana[b], Allan Clemente[a], Jianing Hui[c], John T.S. Irvine[c], H.Q. Nimal Gunaratne[d], Peter K.J. Robertson[d], Christine Edwards[b], Ross N. Gillanders[e], Graham A. Turnbull[e], Linda A. Lawton[b]

[a] Department of Hydraulic and Environmental Engineering, Federal University of Ceará, Fortaleza, Brazil
[b] School of Pharmacy and Life Sciences, Robert Gordon University, Aberdeen, United Kingdom
[c] School of Chemistry, University of St Andrews, St Andrews, United Kingdom
[d] School of Chemistry and Chemical Engineering, Queen's University, Belfast, United Kingdom
[e] Organic Semiconductor Centre, SUPA, School of Physics and Astronomy, University of St Andrews, St Andrews, United Kingdom

ARTICLE INFO

Keywords:
Blue-green algae
Cyanotoxins
Water treatment
Titanium dioxide
Cyanobacteria

ABSTRACT

To date, the high cost of supplying UV irradiation has prevented the widespread application of UV photolysis and titanium dioxide based photocatalysis in removing undesirable organics in the water treatment sector. To overcome this problem, the use of UV-LEDs (365 nm) for photolysis and heterogeneous photocatalysis applying TiO_2 coated glass beads under UV-LED illumination (365 nm) in a pilot scale reactor for the elimination of *Microcystis aeruginosa* PCC7813 and four microcystin analogues (MC-LR, -LY, -LW, -LF) with a view to deployment in drinking water reservoirs was investigated. UV-A (365 nm) photolysis was shown to be more effective than the UV/TiO_2 photocatalytic system for the removal of *Microcystis aeruginosa* cells and microcystins. During photolysis, cell density significantly decreased over 5 days from an initial concentration of 5.8×10^6 cells mL^{-1} until few cells were left. Both intra- and extracellular microcystin concentrations were significantly reduced by 100 and 92 %, respectively, by day 5 of the UV treatment for all microcystin analogues. During UV/TiO_2 treatment, there was great variability between replicates, making prediction of the effect on cyanobacterial cell and toxin behavior difficult.

1. Introduction

Cyanobacterial blooms in freshwater reservoirs represent a threat to human and animal health because of the potential release of a wide variety of harmful metabolites, known collectively as cyanotoxins (Carmichael et al., 2001; Falconer et al., 1983; Jochimsen et al., 1998). Microcystins (MCs) are one of the most commonly reported cyanotoxins with over 247 analogues to date (Spoof and Catherine, 2017). Conventional water treatment (i.e., coagulation, flocculation, sedimentation or flotation and filtration) is used worldwide for treatment of water contaminated with cyanobateria, however, these processes can promote cell rupture and consequently cyanotoxin release into the environment (Chang et al., 2018; Pestana et al., 2019). Further, conventional treatment methods are designed for the removal of suspended or colloidal particles and are not fit to remove dissolved contaminants including dissolved cyanotoxins (Chae et al., 2019; Vilela et al., 2012). In order to mitigate the effect of dissolved cyanobacterial toxins entering water treatment plants, advanced oxidation processes (AOPs) such as photocatalysis and photolysis can be used for the control of cyanobacterial cells and toxic metabolites within reservoirs (Fan et al., 2019; Matthijs et al., 2012; Ou et al., 2011a).

UV photolysis is an AOP that has been widely applied for the inactivation of pathogenic microbes in water treatment and other applications, and can be used as a strategy for removing cyanobacteria and their toxins. A number of studies have evaluated the effects of mainly UV-C (usually 254 nm) and UV-B (usually 312 nm) on microcystin degradation and *Microcystis aeruginosa* removal (Liu et al., 2010; Moon et al., 2017; Tao et al., 2018). This, however, is the first time that the

* Corresponding author. Department of Hydraulic and Environmental Engineering, Federal University of Ceará, Fortaleza, Brazil.
E-mail address: i.de-menezes-castro@rgu.ac.uk (I. Menezes).

https://doi.org/10.1016/j.jenvman.2021.113519
Received 2 March 2021; Received in revised form 14 July 2021; Accepted 7 August 2021
Available online 16 August 2021
0301-4797/© 2021 Elsevier Ltd. All rights reserved.

degradation of *M. aeruginosa* PCC7813 and four microcystin analogues (MC-LR, MC-LW, MC-LY, MC-LF) under UV-A (365 nm) irradiation was investigated.

UV-irradiation-driven titanium dioxide (TiO_2) photocatalysis is another AOP that can be used to control cyanobacteria and their toxins. TiO_2 activation needs to occur under UV light irradiation ($\lambda < 387$ nm) (Chang et al., 2018; Hu et al., 2017; Zhao et al., 2014) due to its wide band gap (3.2 eV and 3.0 eV for the anatase and rutile forms of TiO_2 respectively) (Chen et al., 2015; Hu et al., 2017; Pinho et al., 2015b), which limits its application in drinking water treatment (Jin et al., 2019). UV light is, however, attenuated by water and hence the need for UV irradiation (below 387 nm) is a hurdle in the practical application of photolysis and photocatalysis for water treatment (Chae et al., 2019). To overcome this, and to make the systems practical for application in reservoirs used for drinking water, the system investigated here employs UV (365 nm) light emitting diodes (LEDs), which are low-cost (ca. USD 0.78 per LED), long life (approximately 100,000 working hours; Heering, 2004) and capable of activating TiO_2. In the current study, UV-LED-driven photolysis and TiO_2 photocatalysis were evaluated over 14 days for the elimination of *M. aeruginosa* PCC7813 as well as for the destruction of four microcystin analogues (MC-LR, MC-LW, MC-LY, MC-LF).

2. Methods

2.1. Reagents

The chemicals for artificial fresh water (AFW) and BG-11 culture medium (Stanier et al., 1971) preparation were of reagent grade (Fisher Scientific, UK). AFW was prepared according to Akkanen and Kukkonen (2003) by dissolving $CaCl_2$ (11.8 mg L^{-1}), $MgSO_4$ (4.9 mg L^{-1}), $NaHCO_3$ (2.6 mg L^{-1}) and KCl (0.2 mg L^{-1}) in ultrapure water. For AFW, pH was adjusted to 7 with 1 M hydrochloric acid or 1 M sodium hydroxide if required. Acetonitrile, methanol, and trifluoroacetic acid used for high performance liquid chromatography analysis of microcystins were of HPLC grade (Fisher Scientific, UK). Diuron (3-(3,4-dichlorophenyl)-1, 1-dimethylurea) (Sigma-Aldrich, UK) was used for photosynthetic activity assays. Isoton II Diluent obtained from Beckman Coulter (USA) was used for cyanobacterial cell density determination. All solutions were prepared using ultrapure water (18.2 MΩ) provided by an ELGA PURELAB system (Veolia, UK).

2.2. Cyanobacterial cultivation

The cyanobacterium *M. aeruginosa* PCC7813 (Pasteur Culture Collection) was grown in BG-11 medium at 21 ± 1 °C with constant cool white fluorescent illumination with an average light intensity of 30 μmol photons m^{-2} s^{-1} and constant sparging with sterile air. This strain does not have gas vesicles and produces four main microcystin analogues (MC-LR, MC-LY, MC-LW and MC-LF).

2.3. Reactor design for M. aeruginosa PCC7813 and microcystins treatment

A cell suspension of a 27 days-old culture of *M. aeruginosa* PCC7813 (5×10^6 cells mL^{-1}) in AFW was prepared and sampled prior to addition to the reactors (C_0). The reactors (1000 × 90 mm) were made of a stainless-steel mesh with an aperture of 1.2 × 1.2 mm and 0.4 mm wire strength. Each reactor was placed inside an acrylic cylinder (1100 × 95 mm) that was filled with 6.5 L of *M. aeruginosa* suspension. The acrylic cylinders were sparged from the bases through a multi-porous air-stone with sterile air with the aid of a pump for continuous gentle air flow (1 L min^{-1} per reactor; Fig. S1). The top of the acrylic cylinders was covered with a foam bung to avoid external contamination and to allow air exchanges. The overhead ambient light was of low intensity (2.5 μmol photons m^{-2} s^{-1}). Triplicate reactors were prepared for each of the tested systems (UV-only, TiO_2-only and UV/TiO_2).

One set of three reactors for the UV-A treatment (photolysis) was prepared (Fig. S1A) which consisted of reactors with 5 UV-LED strips (1 m), each with 120 individual UV-LEDs ($\lambda = 365$ nm and light intensity of 5 W m^{-2}), attached to the external surface of the acrylic cylinders and 6.5 L of the cyanobacterial cell suspension added. In the UV-A treatment, empty tetrahedral stainless-steel wire mesh pods (aperture 1.2 × 1.2 mm, wire strength 0.4 mm, Fig. S2) were placed inside the reactors without TiO_2 coated glass beads to allow observation of the effects of only UV-A light on *M. aeruginosa* PCC7813 and its four microcystin analogues. To determine if the TiO_2 coated beads have an effect on the cyanobacterial cells and toxins in the absence of UV light, a second set of triplicate reactors was prepared (Fig. S1B), consisting of 6.5 L of the *M. aeruginosa* PCC7813 suspension and TiO_2 coated glass beads (3.2 g) corresponding to 0.1 % (w/v) TiO_2 inside tetrahedral stainless-steel pods (Fig. S2). The TiO_2 coated beads were manufactured from recycled glass that were prepared as per Pestana et al. (2020) and Hui et al. (2021) containing approximately 12 % (w/w) TiO_2. In the TiO_2-only samples, no UV illumination was used. Finally, a third set of reactors to test the efficacy of TiO_2 photocatalysis was prepared. The UV/TiO_2 treatment consisted of reactors with TiO_2 coated glass beads inside of the stainless-steel pods (Fig. S2), 5 UV-LED strips and 6.5 L of *M. aeruginosa* cell suspension (Fig. S1C). All reactors were maintained in the presence low light intensity (2.5 μmol photons m^{-2} s^{-1}) from overhead lighting since photosynthetic organisms like cyanobacteria require light to survive.

Samples were collected and temperature measured (supplementary material S2) at the same time every day over 14 days. A total of 4 mL was removed at each sampling point, of which 1.5 mL was used for cell enumeration, 1.5 mL was used for intra/extracellular microcystin analysis and 1 mL was used for photosynthetic activity measurements. All aliquots were used immediately except for the aliquots for toxin determination, which were centrifuged for 10 min at 13,000 G and the supernatant and cell pellets were stored separately at −20 °C until further processing and analysis.

2.4. M. aeruginosa PCC7813 regrowth experiment

To assess the regrowth of *M. aeruginosa* PCC7813 after 14 days treatment, samples (50 mL) were removed from each reactor and mixed with an equal volume of BG-11 medium. Aliquots of this mixture (3 mL) were transferred to 28 sterile glass vials (4 mL volume) to allow for sacrificial sampling over seven days with four replicate samples. Samples for each sampling point (i.e., 4 vials) were incubated in a sterile glass beaker (150 mL), covered with a sterile Petri dish lid (Fig. S3). Immediately, one set of samples was removed and cell density was analyzed (C_0 sample), the remaining beakers were incubated at 21 ± 1 °C on a 12/12 h light/dark cycle illuminated by cool white fluorescent lights with an average light intensity of 10.5 μmol photons m^{-2} s^{-1} without agitation for the following 6 days and sampled at the same time every day.

2.5. Analysis

2.5.1. M. aeruginosa PCC7813 cell density determination

M. aeruginosa PCC7813 cell density was measured with a Multisizer 3 (Beckman Coulter, USA). A 50 μm aperture tube was used to detect particle sizes from 1 to 7 μm for both reactor treatments and regrowth experiments. Samples were diluted 200 to 1500-fold in Isoton II Diluent (Beckman Coulter, USA), depending on the sample cell density.

2.5.2. M. aeruginosa PCC7813 photosynthetic activity evaluation

A Mini-PAM system (Walz, Germany) was used for cyanobacterial photosynthetic activity analysis according to Menezes et al. (2020). In short, the minimal fluorescence F_0 was measured by adding 400 μL of sample into a cuvette under agitation followed by diuron (0.5 M)

addition (20 μL) and the true maximal fluorescence measurement (F_M') by a saturating pulse under actinic light. The cyanobacterial photosynthetic activity can be determined by the maximal values of quantum yield of photosystem (PS) II calculated by F_V/F_M', where F_V is the difference between F_M' and F_0 (Stirbet et al., 2018).

2.5.3. Intra- and extracellular microcystin determination by high-performance liquid chromatography (HPLC)

After sampling, the liquid and solid portions of the sample were separated in a centrifuge for 10 min at 13,000 G. The supernatant, representing the extracellular toxin component, was evaporated to dryness in an EZ-II evaporator (Genevac, UK). Dried samples were resuspended in 80 % aqueous methanol (150 μL) and stored at −20 °C until analysis. Cell pellets, representing the intracellular toxin component, were resuspended in 80 % aqueous methanol (150 μL), agitated in a dispersive extractor for 5 min at 2500 rpm and centrifuged for 10 min at 13,000 G to remove cell debris. The resultant supernatant, representing the liberated intracellular content was stored at −20 °C until analysis. The concentrations of four microcystin analogues (MC-LR, MC-LY, MC-LW and MC-LF) were quantified by HPLC (Table 1).

All chromatograms were extracted at 238 nm and quantified using standards (as per Enzo Life Sciences) for calibration between 0.001 and 5 μg mL^{-1} in the Empower software. The limit of quantification was 0.01 μg mL^{-1} for MC-LF and 0.005 μg mL^{-1} for the other microcystin analogues.

2.6. Statistical data analyses

All statistical analyses were performed using RStudio with a significance level of 5 %. In order to verify if the TiO_2-only samples, UV and UV/TiO_2 treatments influenced cell numbers or toxin removal it is necessary to identify a significant reduction of cell density during treatment and intra- and extracellular microcystin concentration (dependent variables) over 14 days (independent variable). The results were pre-analyzed using different statistical models, i.e., linear, piecewise, linear-plato, exponential and logarithmic regression. The models were selected and adjusted using the linear or piecewise regression techniques using the mean of triplicates from each treatment group. The linear or piecewise regression techniques were selected because they were the models that presented the best fit with the data. The mean was selected to create each model because the mean values presented normal distribution according to Shapiro-Wilk Normality Test (data not shown). The linear regression consists in a linear relation between dependent (cell density and microcystins concentration) and independent (time) variables. The piecewise regression consists in multiple linear models to the data for different ranges of the independent variable, which means that the tendency/inclination of the curve of the dependent variable will change over the independent variable. A detailed description of the data analysis and the model selection can be found in the supplementary material (S4).

Table 1
Analytical conditions of HPLC for intra- and extracellular microcystins determination.

Parameters	Conditions
HPLC	2965 separation module and a 2996 photodiode array (PDA) detector (Waters, United States)
Column	Symmetry C18 column, 2.1 mm × 150 mm, 5 μm particle size (Waters, United States)
Mobile phase	A: 0.05 % trifluoroacetic acid in ultrapure water (18.2 MΩ) B: 0.05 % trifluoroacetic acid in acetonitrile
Gradient	Time (min) 0 25 26 29 35 Solvent A (%) 80 30 0 80 80
Flow rate	0.3 mL min^{-1}
Injection volume	35 μL
Column temperature	40 °C
PDA scan range	200–400 nm

3. Results and discussion

3.1. Treatment effects on Microcystis aeruginosa PCC7813 cell density and photosynthetic activity

The removal of *M. aeruginosa* PCC7813 in a photocatalytic and a photolytic reactor using UV-LEDs and TiO_2 coated beads was investigated. The effect of the UV-A treatment presented a piecewise regression tendency (Fig. S4) with a cell density decrease from 5.4×10^6 cells mL^{-1} over 5 days until there were only 1.8×10^4 cells mL^{-1} left (significant tendency rate of 1.12×10^6 cells mL^{-1} day^{-1} until 5 days, $p < 0.01$; Fig. 1A).

Biological replicates can commonly present different behaviors even when exposed to very similar conditions. *M. aeruginosa* PCC7813 cell numbers showed slightly different trends during TiO_2-only treatment with variability increasing as the investigation progressed, particularly after day 10. The outlier observed on day 6 probably occurred due to lack of mixing during cell counting, since samples were consistent until day 10. *M. aeruginosa* PCC7813 cell numbers decreased on average from 5.8×10^6 to 2.6×10^6 cells mL^{-1} with a significant rate of 0.19×10^6 cells mL^{-1} day^{-1} ($p < 0.01$) over 14 days (Fig. 1B) represented by linear regression (Fig. S5). The variability that increased over time might have occurred due to adsorption of cells onto the surface of the TiO_2 layer on the beads and to adhesion of cells onto the inside walls of the reactor.

A reduction in cell numbers was expected to be observed in the UV/TiO_2 treatment on the *M. aeruginosa* PCC7813 cell density based on previous bench-scale studies (Pestana et al., 2020; Chang et al., 2018; Song et al., 2018; Wang et al, 2017, 2018; Pinho et al., 2012). However, the *M. aeruginosa* cell density could best be represented by a piecewise regression tendency (Fig. S6) and significantly rose in the UV/TiO_2 treatment over the first eight days with a tendency rate of 0.46×10^6 cells mL^{-1} day^{-1} ($p < 0.01$), and then decreased after day 8 with a tendency rate of 1×10^6 cells mL^{-1} day^{-1} ($p < 0.01$; Fig. 1C). One possible explanation for this observation is that the TiO_2 coated glass beads have converted some of the incoming UV irradiation into visible light through fluorescence from the semiconductor material (Li et al., 2016) in sufficient quantities to support modest growth, despite the fact that ambient overhead light was of low intensity (2.5 μmol photons m^{-2} s^{-1}) and nominally insufficient for significant cell growth evidenced by no growth observed in the treatments without LEDs (Fig. 1B). Photoluminescence measurements of the TiO_2 coated glass beads show that the beads generate additional visible light, albeit with low efficiency of 7 %. The spectrum was generated at a wavelength of around 430 nm, presenting an overlap with the blue absorption peak of chlorophyll *a*, which can be used by cyanobacteria since chlorophyll *a* has a significant absorbance at this same wavelength and might have contributed to growth of the cyanobacteria (supplementary material S5). It is possible that at the same time cells were receiving sufficient light to grow, during UV/TiO_2 treatment, cells were being damaged and growth was inhibited. Mathew et al. (2012) also observed emission of new wavelengths in the range of visible light (387, 421, 485, 530 and 574 nm) from TiO_2 colloidal nanoparticles after the excitation wavelength of 274 nm. The sample behavior after day 8 is not a true reflection of the individual replicates. After 8 days, the replicate treatments diverged with one of the replicates (Fig. 1C: black) declining rapidly (cell density decreased from 5.8×10^6 to 3.1×10^5 cells mL^{-1}), while the two other replicates (Fig. 1C: red and green) grew, with a cell density increasing from 5.6×10^6 to 7.7×10^6 cells mL^{-1} for one of these replicates (red) and from 5.6 $\times 10^6$ to 8.9×10^6 cells mL^{-1} in the other (green).

In order for the UV illumination to target a specific organism or to activate a catalyst, it must be able to first transmit through the water (Summerfelt, 2003). The lack of cell removal by photocatalysis in two out of three samples during the UV/TiO_2 treatment could be explained by the air flow within the reactor design. In the UV/TiO_2 photocatalytic

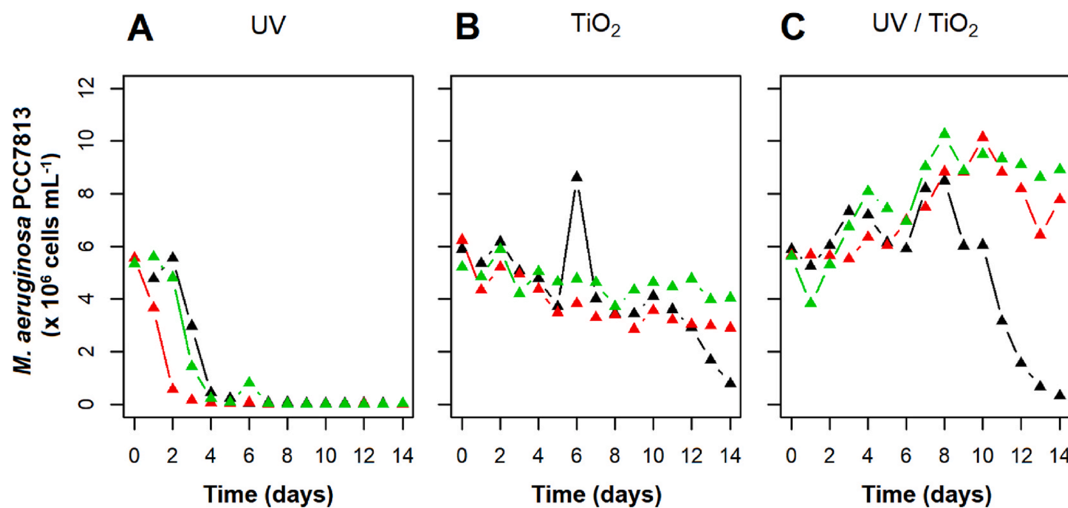

Fig. 1. Effects of (A) UV-LED irradiation (365 nm), (B) TiO_2 coated glass beads under ambient light (2.5 μmol photons m^{-2} s^{-1}) and (C) photocatalytic treatment on *Microcystis aeruginosa* PCC7813 cell density using TiO_2 coated glass beads under UV-LED illumination (365 nm) over 14 days, sparged with sterile air. Data points represent individual replicates for each treatment.

treatment, coated beads inside of the pods may have dispersed the rising air flow into smaller air bubbles, thus attenuating the light to the point where an insufficient number of photons reached the TiO_2 to produce hydroxyl radicals that would be responsible for *M. aeruginosa* PCC7813 removal. The sparging pattern in the reactor where photocatalytic removal of *M. aeruginosa* PCC7813 was observed may have been such that permitted better light penetration, allowing the activation of TiO_2 coated beads by UV illumination and subsequent sufficient hydroxyl radical production.

Direct photolysis and the indirect oxidation by extracellular reactive oxygen species (ROS) initially cause cellular stress and then damage to the cell membrane, without promoting the complete destruction of the cell (Ou et al. 2011a, 2011b, 2011b). Photosynthetic activity as expressed as the F_V/F_M' ratio is a rapid method that can represent the level of stress and/or damage in cyanobacterial cells (Menezes et al., 2020; Stirbet et al., 2018; Yang et al., 2013). Cyanobacterial stress causes a decline in the F_V/F_M' ratio, which means that the lower the F_V/F_M' ratio (photosynthetic activity) the more damage or stress there is to the cyanobacteria. During the UV treatment, cyanobacterial cells suffered inhibition of photosynthetic activity especially at the beginning of the experiment from days 1–4 (Fig. 2A). The photosynthetic activity decrease observed during photolysis corresponds to the decrease in the cell number observed until day 3 (Fig. 1A). As previously reported by Menezes et al. (2020), photosynthetic activity measurements showed a faster response to cell damage than cell density measurements, indicating that cell stress occurred as early as 24 h before cell density changes could be observed by cell density measurements. The cell stress results from day 3 are most likely due to the very low cell density observed from that point in time (5×10^5 cells mL^{-1}), which were lower than the minimum concentration of cells required for cell stress determination. For the TiO_2-only treatment photosynthetic activity remained consistent for the first 6 days (Fig. 2B), remaining at the same level for two out of the three replicates until the end of 14 days (Fig. 2B: red and green). These results support the hypothesis from cell density observations (Fig. 1B) that cells were not inhibited or damaged but were removed from suspension and thus influencing the cell enumeration. Before carrying out the study, UV/TiO_2 treatment was expected to be the most effective treatment through damage to the photosynthetic system of *M. aeruginosa* PCC7813. However, relatively little effect was observed in the UV/TiO_2 treatment over the first 8 days with only one of the

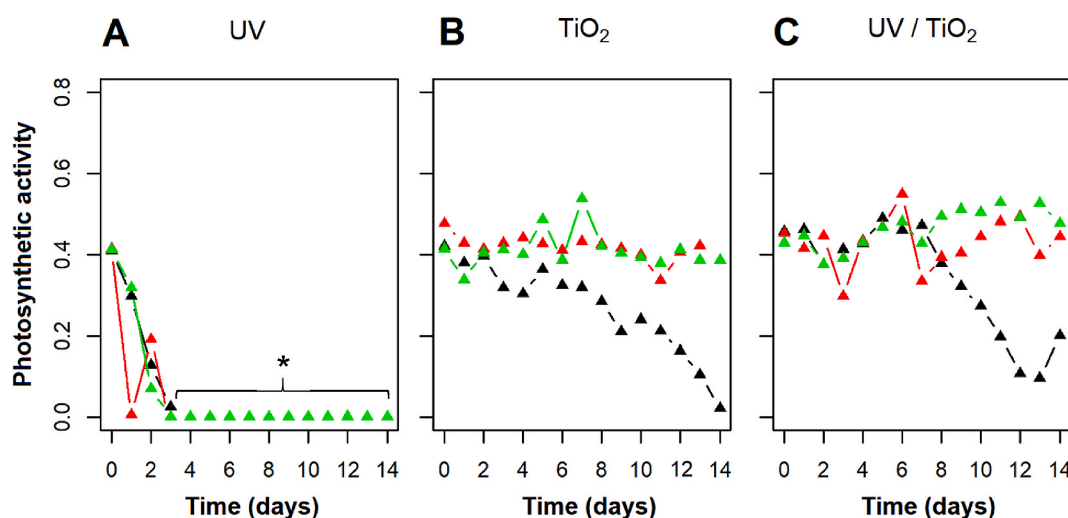

Fig. 2. Effects of (A) UV-LED irradiation (365 nm), (B) TiO_2 coated glass beads under ambient light (2.5 μmol photons m^{-2} s^{-1}) and (C) photocatalytic treatment on *Microcystis aeruginosa* PCC7813 photosynthetic activity using TiO_2 coated glass beads under UV-LED illumination (365 nm) over 14 days under sparging with sterile air. Data points represent replicates from each treatment. *Data points below the limit of quantification as too few cells remained for reliable quantification.

replicates showing a decline in photosynthetic activity from day 7 onwards (Fig. 2C: black) which also corresponds to the cell density decrease in that replicate. (Fig. 1C: black).

An initial decrease of *M. aeruginosa* PCC7813 cell density at the beginning of the experiment was expected which was what had been observed previously in other studies that evaluated *M. aeruginosa* cell density after TiO_2 photocatalytic treatment (Pestana et al., 2020; Chang et al., 2018; Song et al., 2018; Wang et al, 2017, 2018, 2017; Pinho et al., 2012). In particular, the study of Pestana et al. (2020), was a similar experimental design albeit in a smaller bench scale (30 mL of cell suspension and 700 mg of coated beads, equivalent to 0.2 % (w/v) TiO_2). The differences in results between the two studies could be due to the light attenuation of the bubbles being dispersed by the beads.

In the current study, photolysis by UV illumination (365 nm) was observed to be the most effective treatment for *M. aeruginosa* PCC7813 cell destruction. The reduction in the *M. aeruginosa* PCC7813 cell density (Fig. 1A) might be explained by the fact that cyanobacteria do not produce sufficient ROS-scavenging enzymes (e.g., ROS produced by UV treatment; Sinha et al., 2018). ROS oxidize lipids and proteins inside the cyanobacterial cells, resulting in cell wall damage, followed by inactivation of enzymes and ultimately cell death (Sinha et al., 2018). Furthermore, the effect of the UV treatment on *M. aeruginosa* PCC7813 cells might have been caused by indirect oxidation due to intracellular ROS (Ou et al. 2011a, 2011b, 2011b). Intracellular ROS generation may have been enhanced by the presence of intracellular phycocyanin which is a natural cyanobacterial pigment (Robertson et al., 1999). Robertson et al. (1999) suggested that cell destruction can occur from the inside-out rather than the outside-in due to the production of both singlet oxygen and hydroperoxide radical facilitated by the intracellular phycocyanin upon UV-irradiation. After this, the intracellular ROS effects on cells were enhanced by phycocyanin, causing complete degradation of cells. Under UV illumination alone, phycocyanin can contribute to the degradation of cells by two mechanisms: firstly, during the electron transfer process (Equation (1)), the photoexcited phycocyanin transfers an electron to oxygen, producing the superoxide radical that then becomes a hydroperoxide radical by protonation. Secondly, during the energy transfer process (Equation (2)), phycocyanin and oxygen interact to produce singlet oxygen (Robertson et al., 1999) with both ROS attacking the cell structures from within.

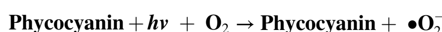

$$\textbf{Phycocyanin} + h\nu + O_2 \rightarrow \textbf{Phycocyanin} + \bullet O_2^-$$

$$\bullet O_2^- + H^+ \rightarrow \bullet OOH \quad (1)$$

$$\textbf{Phycocyanin} + h\nu + O_2 \rightarrow \textbf{Phycocyanin} + {}^1O_2 \quad (2)$$

Furthermore, cyanobacteria release oxygen during photosynthesis which can interact with UV light and other organic compounds to produce ROS (Pattanaik et al., 2007). The ROS produced by UV-A illumination in the present study might also be responsible for damaging *M. aeruginosa* PCC7813 cells.

UV-C (254 nm) has been widely applied as a germicide for the inactivation of bacteria and viruses by denaturing the DNA of microorganisms and causing death or function loss (Boyd et al., 2020; Summerfelt, 2003). However, it is likely that the UV-A illumination (365 nm) used in the present study was able to destroy *M. aeruginosa* PCC7813 cells due to the generation of ROS and the presence of phycocyanin inside the cyanobacterial cells. Therefore, unlike UV-C illumination, UV-A illumination might be specific to cyanobacterial control and it may not affect other phytoplankton such as diatoms or green algae, although this requires further confirmation. The specificity of the effects of the UV-A photolysis on cyanobacteria would impact the phytoplankton community in natural waterbodies less than the application of UV-B/UV-C photolysis. At the same time, having the additional advantage of presenting with lower capital cost. Previous studies have investigated the application of other treatments (e.g., hydrogen peroxide oxidation) and observed that some treatment were selective for cyanobacterial species due to their biochemistry (Drábková et al., 2007a, 2007b; Matthijs et al., 2012). Ou et al. (2011a, 2011b) pointed out that the UV-C-induced damage occurs via either direct photolysis or indirect oxidation by intra- and/or extracellular ROS. UV irradiation causes damage to the photosynthesis system, including PS I, PS II and phycobilisome which interrupts the electron transport chain and retards the critical reactions during photosynthesis, followed by the decomposition of cytoplasmic inclusions and finally cell destruction with release of intracellular organic matter. The same mechanisms might have occurred during the present UV-A photolysis where the photosynthetic system of *M. aeruginosa* PCC7813 was affected (Fig. 2A) and cellular destruction occurred due to intracellular ROS (Fig. 1A). Yang et al. (2015) evaluated the effects of high-energy UV-B illumination (280–320 nm) on a toxic (FACHB 915) and a non-toxic (FACHB 469) strain of *M. aeruginosa* photosynthetic activity. The UV-B irradiation resulted in an inhibition of the photosynthetic activity of both toxic and non-toxic strains over 3 days of exposure due to damage to photosystem II (Yang et al., 2015). However, both *M. aeruginosa* strains used by Yang et al. (2015) showed signs of photosynthetic activity recovery at the end of the experiment.

3.2. Intra- and extracellular microcystin removal

The intracellular microcystin concentration for all analogues diminished significantly in a piecewise regression tendency (Fig. S7 – S10) over the first 5 days of the UV treatment (Fig. 3A) with the complete removal of all microcystin analogues by this time (approximate rate of 40, 22, 15 and 2.6 ng mL^{-1} day^{-1} of intracellular MC-LR, MC-LF, MC-LW and MC-LY, respectively, $p < 0.01$ for all samples). The decrease of all four analogues of intracellular microcystins during UV treatment (Fig. 3A) corresponds to the reduction of *M. aeruginosa* cell density and subsequent microcystins leak (Fig. 1A). For the TiO_2-only samples (Fig. 3B), the mean values suggest removal of 20, 43, 42 and 42 % of intracellular MC-LR, MC-LF, MC-LW and MC-LY, respectively, or a significant decrease in a linear regression rate (Fig. S11 – S14) of 3.7, 2.8, 2.9 and 0.3 ng mL^{-1} day^{-1} (for all samples $p < 0.05$) over 14 days. Samples remained consistent over the first 11 days, however, it was possible to observe divergence in the results in the later stages. During UV/TiO_2 treatment, intracellular microcystins samples presented high variability over 14 days (Fig. 3C) and while one replicate (Fig. 3C: black) showed complete removal of all microcystins at the end of the experiment, another replicate (Fig. 3C: green) demonstrated microcystins concentration of 157, 74, 59 and 11 ng mL^{-1} for MC-LR, MC-LF, MC-LW and MC-LY respectively. It is noteworthy that across all the treatments all microcystin analogues behaved in a similar manner (Fig. 3), for example, one replicate during the UV treatment (Fig. 3A: red) all analogues decreased on day 2, followed by the other two replicates on day 4 (Fig. 3A: green and black). Variability in the toxin concentrations observed in Fig. 3C is a further indication that both cell lysis due to UV/TiO_2 and cell growth due to the production of visible light are acting in the system.

For the UV treatment, all microcystins per cell were undetectable after 6 days (Fig. 4A). The complete destruction of cells during photolysis (Fig. 1A) could be confirmed by this corresponding decrease in the toxin ratio (i.e., toxin concentration per cell number). For TiO_2-only samples, the toxin concentration per cell presented variability (Fig. 4B). Despite the slight decrease in cell number of TiO_2-only samples, no cell stress was detected when analyzing both photosynthetic activity (Fig. 2B) and intracellular toxin (Fig. 3B), indicating that cells were not actually damaged and/or dead but there was physical cell removal of intact healthy cells by adsorption of cells onto the surface of the TiO_2 beads and the surface of the reactors.

The amount of toxin per cell over 14 days in the UV/TiO_2 treatment diminished by 54, 64, 70 and 72 % for MC-LR, -LY, -LW and -LF, respectively (Fig. 4C). One reason for the reduction in the toxin concentration per cell could be that some of the *M. aeruginosa* PCC7813 cells

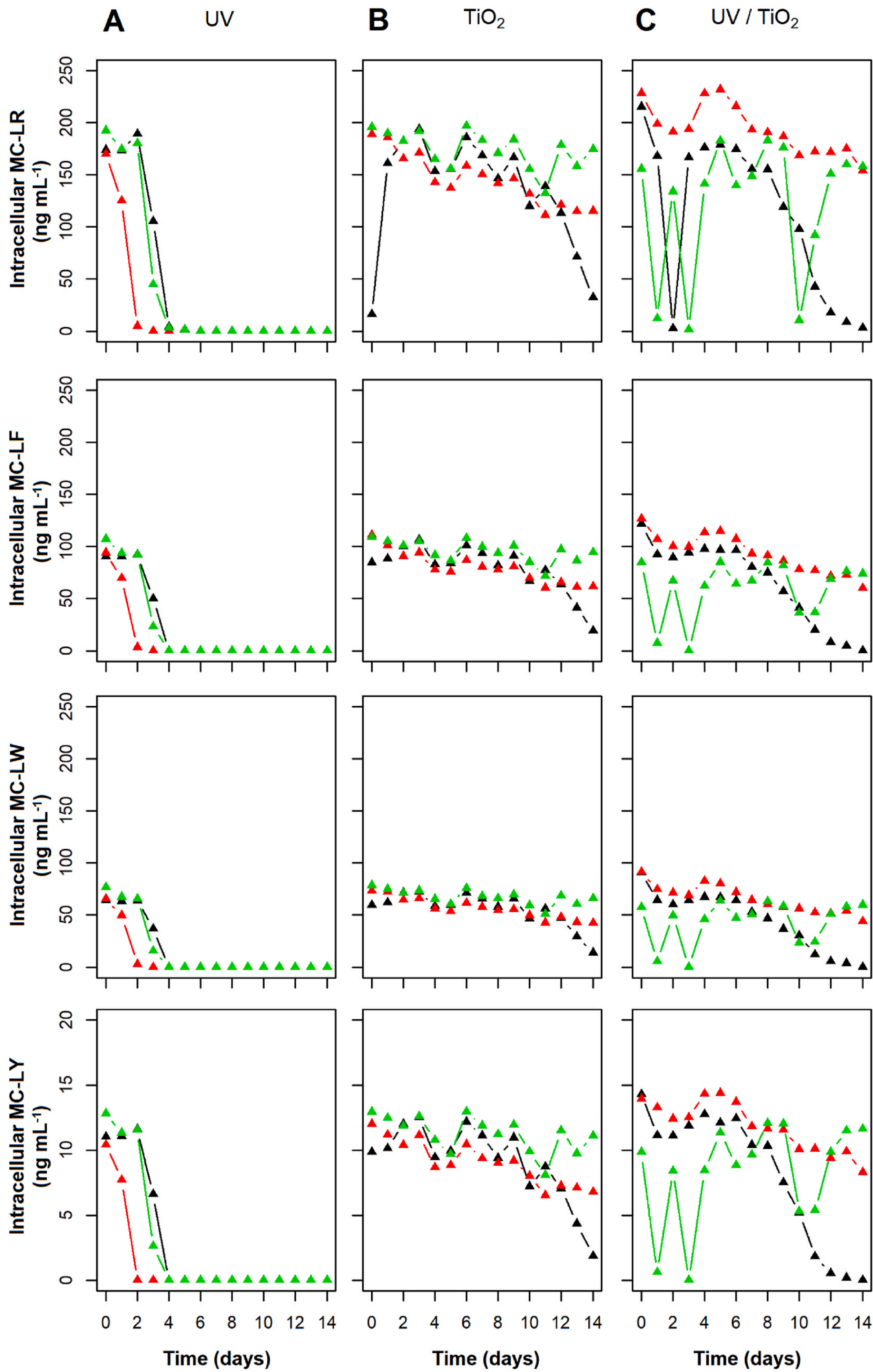

Fig. 3. Intracellular microcystin concentrations produced by *Microcystis aeruginosa* PCC7813 during (A) UV, (B) TiO_2 under ambient light (2.5 μmol photons m^{-2} s^{-1}) and (C) UV/TiO_2 treatment over 14 days under constant agitation. Data points represent replicates from each treatment.

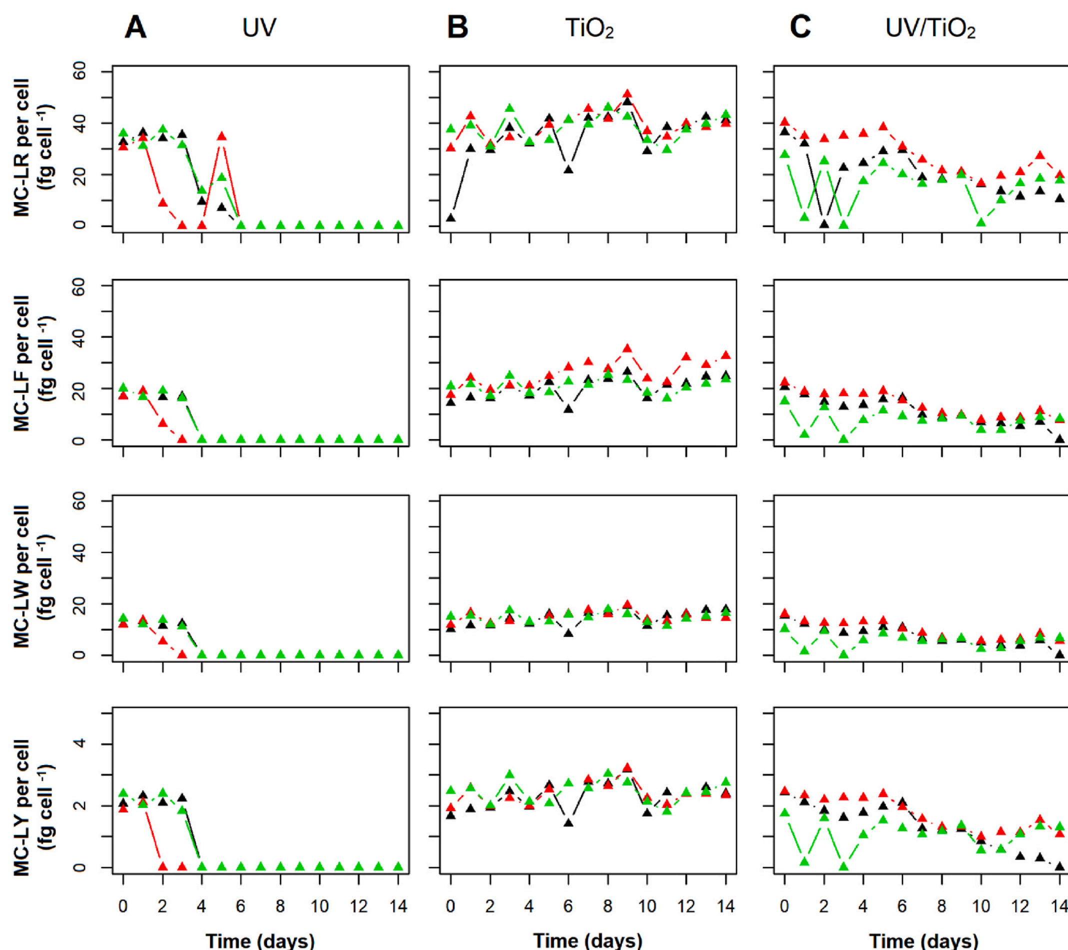

Fig. 4. Intracellular microcystin analogues ratio (toxin $cell^{-1}$) in *Microcystis aeruginosa* PCC7813 over 14 days of (A) UV, (B) TiO_2 under ambient light (2.5 μmol photons m^{-2} s^{-1}) and (C) UV/TiO_2 treatment under constant agitation. Data points represent replicates from each treatment.

were detected and counted as living organisms, however, some of the cells were probably fragmented and inactive. Additionally, as was previously mentioned, intracellular microcystin could leak the cell if the cell wall was compromised. Another reason for the decrease in toxin concentration could be microcystins binding to intracellular proteins which *M. aeruginosa* is known to do as demonstrated by Zilliges et al. (2011). Pestana et al. (2020) also observed a reduction in the toxin per cell ratio of the same intracellular microcystin analogues used in the present study (MC-LR, -LY, -LW and -LF) TiO_2 coated glass beads under UV/LED illumination (365 nm, 2.1 mW s^{-1}), which they ascribed to microcystins binding to intracellular proteins.

Microcystins are commonly released into the surrounding water after cell rupture by water treatment processes. Therefore, water treatment technologies must be applied to remove toxins that are released into the water since conventional treatment cannot remove dissolved components (Chow et al., 1999). After the liberation of intracellular microcystins during the UV treatment, samples could be best represented by a piecewise regression (Fig. S19 – S22) with removal for all extracellular microcystins amounting to 92 % for MC-LR and complete removal of the other three analogues over the first 5 days (Fig. 5A). The reduction in *M. aeruginosa* PCC7813 cell number (Fig. 1A) is the most likely reason for the decrease of intracellular microcystins during the UV treatment (Fig. 3A) due to cell lysis and release of the intracellular content to the surrounding water followed by the immediate removal of the extracellular microcystins by direct photolysis and indirect oxidation of ROS (Fig. 5A). No significant change ($p > 0.05$) in the extracellular concentration of any of the microcystin analogues was observed over 14 days in the TiO_2-only samples (Fig. 5B), indicating that there was no microcystins release from the cells. This finding also corroborates the theory that cells were not destroyed in TiO_2-only samples and remained intact. During UV/TiO_2 treatment, there was no increase in the extracellular microcystin concentrations for most samples over 14 days (Fig. 5C: red and green). However, the cell reduction observed for one of the replicates (Fig. 2C: black) and the decline of intracellular microcystins (Fig. 3C: black) of this replicate in the UV/TiO_2 treatment could account for the increase of extracellular microcystins (Fig. 5C: black). The toxin concentration released in this replicate (Fig. 5C: black) corresponds to the concentration increase of the extracellular microcystins, an indication of cell lysis caused by the UV/TiO_2.

A study by Robertson et al. (1999) evaluated the destruction of MC-LR under UV/TiO_2 photocatalysis and photolysis in the presence of phycocyanin. The authors also observed a decline of MC-LR concentration when the sample was treated with only UV-A light in the presence of phycocyanin, corroborating the results of the current study. However, when no phycocyanin was present, the UV light had no effect on the toxin degradation, showing that phycocyanin acts as a photocatalyst for microcystin destruction under UV illumination until the pigment was completely bleached (Robertson et al., 1999). There is a number of studies which have investigated the effects of UV illumination on microcystins (Liu et al., 2010; Pinho et al, 2012, 2015a, 2015b, 2015b; Triantis et al., 2012), however, the breakdown of pure microcystin requires UV-C. In order for the UV-A illumination used in the current study to breakdown microcystins, the presence of phycocyanin is necessary. Similar effects were observed by Rinalducci et al. (2008) which demonstrated the photosensitizing effect of phycocyanin on the phycobilisomes of another cyanobacterium (Synechocystis PCC 6803).

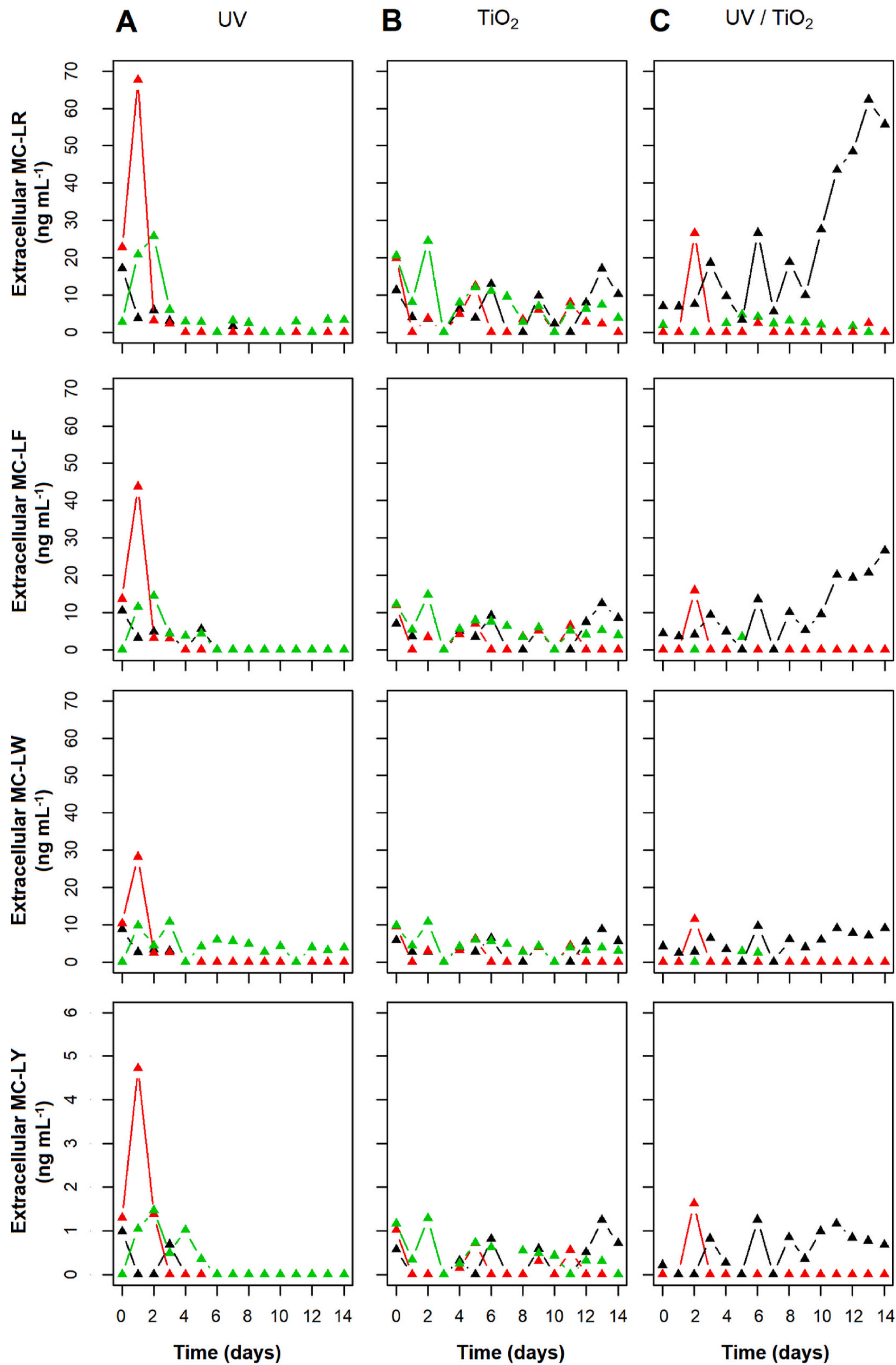

Fig. 5. Extracellular microcystin analogue concentrations produced by *Microcystis aeruginosa* PCC7813 during (A) UV, (B) TiO_2 under ambient light (2.5 μmol photons m^{-2} s^{-1}) and (C) UV/TiO_2 treatment over 14 days under constant agitation. Data points represent replicates from each treatment.

Pestana et al. (2020) carried out a bench-scale (30 mL of cell suspension) study of the destruction *M. aeruginosa* strain (PCC7813) (MC-LR, -LY, -LF and -LW) under UV/TiO_2 photocatalysis the TiO_2 coated beads used in the current study. Intracellular microcystin analogues were removed by 49 % and extracellular microcystins that were release after cell lysis were completely removed by UV/TiO_2 photocatalysis. Similar results were expected in the current study, however, UV photolysis was more efficient for the removal of microcystins than the UV/TiO_2 photocatalytic treatment used in the present study. The difference in the results might have occurred due to the larger scale and lower initial cell concentration (6.5 L with 5×10^6 cells mL^{-1} in the current study compared to 30 mL with 15×10^6 cells mL^{-1} used in Pestana et al. (2020) study). Further, in the current study, a small amount of cell growth was observed in UV/TiO_2 treatment over the first 8 days (Fig. 1C). Additionally, stronger mixing caused by the multi-porous air-stone in the base of the reactor in the current study combined with the dispersion of the larger air bubbles by the TiO_2-coated glass beads that potentially attenuated the effects of the UV irradiation, rendering the UV/TiO_2 treatment less effective. In contrast, in the Pestana et al. (2020) study, only very gentle single point sparging (flow rate of 1.5 L min^{-1}) was used from the top of the vials. Finally, the shadowing effect caused by the coated glass beads and the stainless-steel pods inside the reactors (which were not used in the Pestana et al. (2020) study) may have interfered in the efficiency of the photocatalytic removal of the microcystins.

3.3. *Microcystis aeruginosa PCC7813 regrowth post UV and UV/TiO_2 treatment*

It is important to evaluate cyanobacterial regrowth potential to determine the residual effects of the treatment. For the UV-A treated cells the difference in cell concentration between the beginning of the regrowth experiment and day 6 was not significant ($p = 0.08$) due to the fact that few cells remained viable after UV treatment that were not inhibited/damaged (Fig. 6A). The remaining *M. aeruginosa* PCC7813 cells had a doubling rate of 1.9 days over 6 days of regrowth (Fig. 6A), which is still considered a typical doubling rate for *M. aeruginosa*. For the TiO_2-only samples, variability was high, with one of the replicates (Fig. 6B: black) which had the lowest cell density after 14 days treatment with TiO_2-only showing no regrowth. This replicate (Fig. 6B: black) actually showed a decreased in cell density from 4.1×10^5 to 2.5×10^5 cells mL^{-1} over 6 days, while the other two replicates (Fig. 6B: red and green) presented a doubling rate of 2.9 and 3.8 days, respectively. The same sample variability was observed in regrowth samples from the UV/TiO_2 treatment (Fig. 6C). While cell concentrations in two replicates (Fig. 6C: black and green) doubled at a rate of 4.2 and 4.7 days respectively, the third replicates (Fig. 6C: red) decreased in cell density from 4.1×10^6 to 1.4×10^5 cells mL^{-1} over 6 days.

Wilson et al. (2006) stated an average doubling rate for 32 strains of *Microcystis* cultured in BG-11 medium as 2.8 days. Some UV treatment samples from the current study presented a faster doubling rate of 1.9 days and some UV/TiO_2 treatment samples showed a slower doubling rate of 4.2 and 4.7 days.

Despite the lower initial cell density after 6 days of regrowth in UV treatment (Fig. 6A), the cells in UV treatment showed the fastest doubling rate (1.9 days) when compared to cells from TiO_2-only samples and UV/TiO_2 treatment (Fig. 6B and C), as previously observed by Dunn and Manoylov (2016). In the UV treatment, low cell density means low competition for resources, hence this is often when growth is fastest.

Ou et al. (2012) studied the effects of different UV-C dosages (140–4200 mJ cm^{-2}) on *M. aeruginosa* FACHB-912 recovery over 7 days. They found a significant reduction in indicators of photosynthesis (e.g., quantum yield) and chlorophyll *a* for samples irradiated at 350, 700, 1400 and 4200 mJ cm^{-2}, showing the irreversible inhibition of the photosynthetic system in the *M. aeruginosa* cells FACHB-912 after UV-C irradiation which then inhibited the reproduction and recovery of *M. aeruginosa* cells (Ou et al., 2012).

A study by Huang et al. (2011) evaluated the regrowth potential of *M. aeruginosa* after 24 h of ZnO/γ-Al_2O_3 photocatalytic treatment under solar light. After 12 days of regrowth, the cell density of treated samples was less than 85 % of that of the control, highlighting the lasting effect of photocatalysis on *M. aeruginosa* cells even though a different type of photocatalyst and irradiation was applied (Huang et al., 2011).

4. Conclusion

The current study investigated the effects of UV-A photolysis and a UV/TiO_2 photocatalytic system using TiO_2 coated glass beads on *M. aeruginosa* PCC7813 cells and the four main microcystin analogues (MC-LR, -LY, -LW and -LF) this strain produces. Both systems had energy-efficient UV illumination supplied by UV-LEDs for cyanobacteria and cyanotoxin control. The UV photolysis was able to consistently remove cyanobacterial cells and toxins, and therefore was shown to be more effective than the UV/TiO_2 photocatalytic system which gave a delayed removal of cells and concerningly, slightly supported growth in the first 8 days. All the data analysis (cell density, photosynthetic

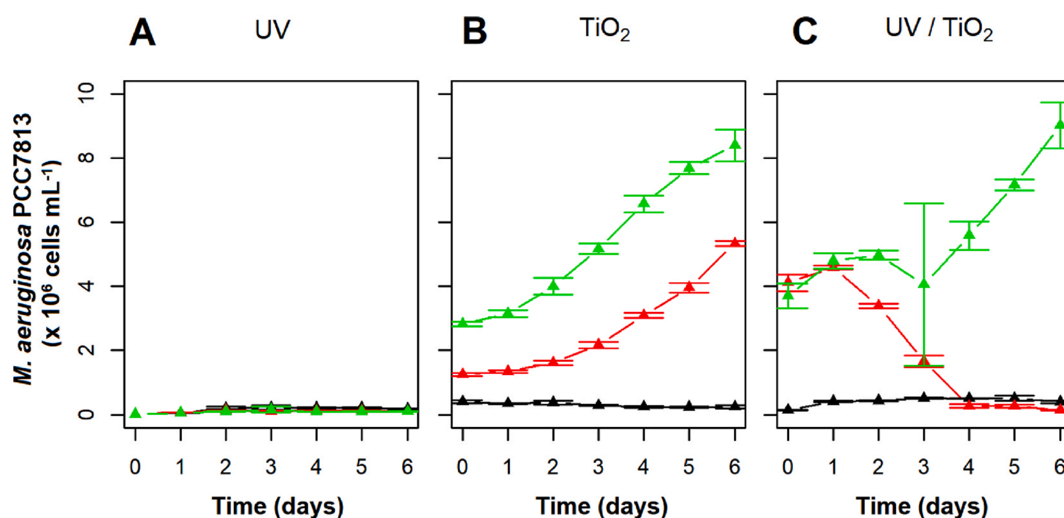

Fig. 6. Effects of (A) UV-LED irradiation (365 nm), (B) TiO_2 coated glass beads under ambient light (2.5 μmol photons m^{-2} s^{-1}) and (C) photocatalytic treatment on *Microcystis aeruginosa* PCC7813 regrowth using TiO_2 coated glass beads under UV-LED illumination (365 nm) over seven days under cool white fluorescent lights of 10.5 μmol photons m^{-2} s^{-1}. Data points represent replicates from each treatment ($n = 4$).

activity, toxin per cell, intra- and extracellular toxin) indicate that UV-A photolysis was capable of not only inhibiting *M. aeruginosa* PCC7813 cells, but it significantly damaged them to the point that only a very limited regrowth was observed. An advantage of using UV-A irradiation over other types of UV irradiation is that UV-A illumination might be specific to cyanobacterial control due to the presence of phycocyanin inside of the cyanobacterial cells. To confirm this, the effects of UV photolysis on other phytoplankton (diatoms and green algae) and cyanobacterial species shouldbe investigated, such as a mesocosms experiment with community analysis. An additional advantage of employing UV-A over other types of UV irradiation is that lamps generating UV-A tend to be more economical in terms of capital cost compared to UV-B or UV-C generating lamps. In practice, many aspects of the reactor design need to be optimized and field-tested to allow *in-situ* application inside reservoirs: vertical or horizontal orientation of reactors, optimization of the active surface area and contact time, incorporation of waterproof UV-LEDs, and powering the units *in-situ* exploring solar options. The current study has successfully demonstrated that UV-LED-based advanced oxidation techniques could be operated at a larger-than-bench scale and control cyanobacteria and their toxins.

Declaration of competing interest

The authors declare that they have no known competing financial interests or personal relationships that could have appeared to influence the work reported in this paper.

Acknowledgements

The authors would like to thank the Engineering and Physical Sciences Research Council (EPSRC) [EP/P029280/1], the Coordination for the Improvement of Higher Education Personnel - CAPES [PROEX 20/2016 and PrInt 88887.311806/2018–00], and the Brazilian National Research Council – CNPq [403116/2016–3 and 304164/2017–8] for funding this research. As per EPSRC requirement all data will be made publicly available via the Robert Gordon University's open access repository OpenAIR@RGU. Further, the first author also acknowledges the scholarship from the Brazilian National Research Council - CNPq. Finally, Len Montgomery is appreciated for proof-reading the manuscript and the authors would like to thank Dr Nathan Skillen of Queen's University Belfast, for help and guidance with the electrical wiring of the LEDS for the reactors.

Appendix A. Supplementary data

Supplementary data to this article can be found online at https://doi.org/10.1016/j.jenvman.2021.113519.

Credit author statement

Indira Menezes – Investigation, Writing – original draft, Visualization, Data curation. José Capelo-Neto – Conceptualization, Supervision, Funding acquisition. Carlos J. Pestana – Conceptualization, Investigation, Writing – review & editing, Supervision, Project administration. Allan Clemente – Formal analysis, Visualization. Jianing Hui – Writing – review & editing, Resources. John T. S. Irvine – Conceptualization, Resources, Funding acquisition. H.Q. Nimal Gunaratne – Writing – review & editing, Resources. Peter K.J. Robertson – Conceptualization, Funding acquisition. Christine Edwards – Methodology, Resources, Ross N. Gillanders – Investigation, Resources. Graham A. Turnbull – Investigation, Resources. Linda A. Lawton – Conceptualization, Writing – review & editing, Supervision, Funding acquisition.

References

Akkanen, J., Kukkonen, J.V.K., 2003. Measuring the bioavailability of two hydrophobic organic compounds in the presence of dissolved organic matter. Environ. Toxicol. Chem. 22, 518–524.

Boyd, B., Suslov, S.A., Becker, S., Greentree, A.D., Maksymov, I.S., 2020. Beamed UV sonoluminescence by aspherical air bubble collapse near liquid-metal microparticles. Sci. Rep. 10, 1–8. https://doi.org/10.1038/s41598-020-58185-2.

Carmichael, W.W., Azevedo, S.M.F.O., An, J.S., Molica, R.J.R., Jochimsen, E.M., Lau, S., Rinehart, K.L., Shaw, G.R., Eaglesham, G.K., 2001. Human fatalities from cyanobacteria: chemical and biological evidence for cyanotoxins. Environ. Health Perspect. 109, 663–668. https://doi.org/10.1289/ehp.01109663.

Chae, S., Noeiaghaei, T., Oh, Y., Kim, I.S., Park, J.S., 2019. Effective removal of emerging dissolved cyanotoxins from water using hybrid photocatalytic composites. Water Res. 149, 421–431. https://doi.org/10.1016/j.watres.2018.11.016.

Chang, C.W., Huo, X., Lin, T.F., 2018. Exposure of *Microcystis aeruginosa* to hydrogen peroxide and titanium dioxide under visible light conditions: modeling the impact of hydrogen peroxide and hydroxyl radical on cell rupture and microcystin degradation. Water Res. 141, 217–226. https://doi.org/10.1016/j.watres.2018.05.023.

Chen, L., Zhao, C., Dionysiou, D.D., O'Shea, K.E., 2015. TiO_2 photocatalytic degradation and detoxification of cylindrospermopsin. J. Photochem. Photobiol. Chem. 307–308, 115–122. https://doi.org/10.1016/j.jphotochem.2015.03.013.

Chow, C.W.K., Drikas, M., House, J., Burch, M.D., Velzeboer, R.M.A., 1999. The impact of conventional water treatment processes on cells of the cyanobacterium *Microcystis aeruginosa*. Water Res. 33, 3253–3262. https://doi.org/10.1016/S0043-1354(99)00051-2.

Drábková, Michaela, Admiraal, W., Maršálek, B., 2007a. Combined exposure to hydrogen peroxide and light-selective effects on cyanobacteria, green algae, and diatoms. Environ. Sci. Technol. 41, 309–314. https://doi.org/10.1021/es060746i.

Drábková, M., Matthijs, H.C.P., Admiraal, W., Maršálek, B., 2007b. Selective effects of H_2O_2 on cyanobacterial photosynthesis. Photosynthetica 45, 363–369. https://doi.org/10.1007/s11099-007-0062-9.

Dunn, R.M., Manoylov, K.M., 2016. The effects of initial cell density on the growth and proliferation of the potentially toxic cyanobacterium *Microcystis aeruginosa*. J. Environ. Protect. 7, 1210–1220. https://doi.org/10.4236/jep.2016.79108.

Falconer, I.R., Beresford, A.M., Runnegar, M.T., 1983. Evidence of liver damage by toxin from a bloom of the blue-green alga, *Microcystis aeruginosa*. Med. J. Aust. 1, 511–514. https://doi.org/10.5694/j.1326-5377.1983.tb136192.x.

Fan, F., Shi, X., Zhang, M., Liu, C., Chen, K., 2019. Comparison of algal harvest and hydrogen peroxide treatment in mitigating cyanobacterial blooms via an *in situ* mesocosm experiment. Sci. Total Environ. 694, 133721. https://doi.org/10.1016/j.scitotenv.2019.133721.

Heering, W., 2004. UV-sources - basics, properties and applications. Int. Ultrav. Assoc. 6, 7–13.

Hu, Xi, Hu, Xinjiang, Tang, C., Wen, S., Wu, X., Long, J., Yang, X., Wang, H., Zhou, L., 2017. Mechanisms underlying degradation pathways of microcystin-LR with doped TiO_2 photocatalysis. Chem. Eng. J. 330, 355–371. https://doi.org/10.1016/j.cej.2017.07.161.

Huang, W.J., Lin, T.P., Chen, J.S., Shih, F.H., 2011. Photocatalytic inactivation of cyanobacteria with ZnO/γ-Al_2O_3 composite under solar light. J. Environ. Biol. 32, 301–307.

Hui, J., Pestana, C.J., Caux, M., Gunaratne, H.Q.N., Edwards, C., Robertson, P.K.J., Lawton, L.A., Irvine, J.T.S., 2021. Graphitic-C_3N_4 coated floating glass beads for photocatalytic destruction of synthetic and natural organic compounds in water under UV light. J. Photochem. Photobiol. Chem. 405, 112935. https://doi.org/10.1016/j.jphotochem.2020.112935.

Jin, Y., Zhang, S., Xu, H., Ma, C., Sun, J., Li, H., 2019. Application of N-TiO_2 for visible-light photocatalytic degradation of *Cylindrospermopsis raciborskii*. More difficult than that for photodegradation of *Microcystis aeruginosa*? Environ. Pollut. 245, 642–650. https://doi.org/10.1016/j.envpol.2018.11.056.

Jochimsen, E., Carmichael, W.W., An, J., Cardo, D.M., Cookson, S.T., Holmes, C.E.M., Antunes, B.C., Melo Filho, D.A., Lyra, T.M., Barreto, V.S.T., Azevedo, S.M.F.O., Jarvis, W., 1998. Liver failure and death after exposure to microcystins. N. Engl. J. Med. 338, 873–878. https://doi.org/10.1080/13504509.2013.856048 M4 - Citavi.

Li, L., Sahi, S.K., Peng, M., Lee, E.B., Ma, L., Wojtowicz, J.L., Malin, J.H., Chen, W., 2016. Luminescence-and nanoparticle-mediated increase of light absorption by photoreceptor cells: converting UV light to visible light. Sci. Rep. 6 https://doi.org/10.1038/srep20821.

Liu, X., Chen, Z., Zhou, N., Shen, J., Ye, M., 2010. Degradation and detoxification of microcystin-LR in drinking water by sequential use of UV and ozone. J. Environ. Sci. 22, 1897–1902. https://doi.org/10.1016/S1001-0742(09)60336-3.

Mathew, S., Kumar Prasad, A., Benoy, T., Rakesh, P.P., Hari, M., Libish, T.M., Radhakrishnan, P., Nampoori, V.P.N., Vallabhan, C.P.G., 2012. UV-visible photoluminescence of TiO_2 nanoparticles prepared by hydrothermal method. J. Fluoresc. 22, 1563–1569. https://doi.org/10.1007/s10895-012-1096-3.

Matthijs, H.C.P., Visser, P.M., Reeze, B., Meeuse, J., Slot, P.C., Wijn, G., Talens, R., Huisman, J., 2012. Selective suppression of harmful cyanobacteria in an entire lake with hydrogen peroxide. Water Res. 46, 1460–1472. https://doi.org/10.1016/j.watres.2011.11.016.

Menezes, I., Maxwell-mcqueeney, D., Pestana, C.J., Edwards, C., Lawton, L.A., 2020. Oxidative stress in the cyanobacterium *Microcystis aeruginosa* PCC 7813 : comparison of different analytical cell stress detection assays. Chemosphere 269, 128766. https://doi.org/10.1016/j.chemosphere.2020.128766.

Moon, B.R., Kim, T.K., Kim, M.K., Choi, J., Zoh, K.D., 2017. Degradation mechanisms of Microcystin-LR during UV-B photolysis and UV/H_2O_2 processes: byproducts and

pathways. Chemosphere 185, 1039–1047. https://doi.org/10.1016/j.chemosphere.2017.07.104.

Ou, H., Gao, N., Deng, Y., Qiao, J., Wang, H., 2012. Immediate and long-term impacts of UV-C irradiation on photosynthetic capacity, survival and microcystin-LR release risk of *Microcystis aeruginosa*. Water Res. 46, 1241–1250. https://doi.org/10.1016/j.watres.2011.12.025.

Ou, H., Gao, N., Deng, Y., Qiao, J., Zhang, K., Li, T., Dong, L., 2011a. Mechanistic studies of *Microcystic aeruginosa* inactivation and degradation by UV-C irradiation and chlorination with poly-synchronous analyses. DES 272, 107–119. https://doi.org/10.1016/j.desal.2011.01.014.

Ou, H., Gao, N., Deng, Y., Wang, H., Zhang, H., 2011b. Inactivation and degradation of *Microcystis aeruginosa* by UV-C irradiation. Chemosphere 85, 1192–1198. https://doi.org/10.1016/j.chemosphere.2011.07.062.

Pattanaik, B., Schumann, R., Karsten, U., 2007. Effects of ultraviolet radiation on cyanobacteria and their protective mechanisms. Limnology 29–45.

Pestana, C.J., Capelo-Neto, J., Lawton, L., Oliveira, S., Carloto, I., Linhares, H.P., 2019. The effect of water treatment unit processes on cyanobacterial trichome integrity. Sci. Total Environ. 659, 1403–1414. https://doi.org/10.1016/j.scitotenv.2018.12.337.

Pestana, C.J., Portela Noronha, J., Hui, J., Edwards, C., Gunaratne, H.Q.N., Irvine, J.T.S., Robertson, P.K.J., Capelo-Neto, J., Lawton, L.A., 2020. Photocatalytic removal of the cyanobacterium *Microcystis aeruginosa* PCC7813 and four microcystins by TiO_2 coated porous glass beads with UV-LED irradiation. Sci. Total Environ. 745, 141154. https://doi.org/10.1016/j.scitotenv.2020.141154.

Pinho, L.X., Azevedo, J., Brito, A., Santos, A., Tamagnini, P., Vilar, V.J.P., Vasconcelos, V.M., Boaventura, R.A.R., 2015a. Effect of TiO_2 photocatalysis on the destruction of *Microcystis aeruginosa* cells and degradation of cyanotoxins microcystin-LR and cylindrospermopsin. Chem. Eng. J. 268, 144–152. https://doi.org/10.1016/j.cej.2014.12.111.

Pinho, L.X., Azevedo, J., Miranda, S.M., Ângelo, J., Mendes, A., Vilar, V.J.P., Vasconcelos, V., Boaventura, R.A.R., 2015b. Oxidation of microcystin-LR and cylindrospermopsin by heterogeneous photocatalysis using a tubular photoreactor packed with different TiO_2 coated supports. Chem. Eng. J. 266, 100–111. https://doi.org/10.1016/j.cej.2014.12.023.

Pinho, L.X., Azevedo, J., Vasconcelos, V.M., Vilar, V.J.P., Boaventura, R.A.R., 2012. Decomposition of *Microcystis aeruginosa* and microcystin-LR by TiO_2 oxidation using artificial UV light or natural sunlight. J. Adv. Oxid. Technol. 15, 98–106. https://doi.org/10.1515/jaots-2012-0111.

Rinalducci, S., Pedersen, J.Z., Zolla, L., 2008. Generation of reactive oxygen species upon strong visible light irradiation of isolated phycobilisomes from *Synechocystis* PCC 6803. Biochim. Biophys. Acta Bioenerg. 1777, 417–424. https://doi.org/10.1016/j.bbabio.2008.02.005.

Robertson, P.K.J., Lawton, L.A., Cornish, B.J.P.A., 1999. The involvement of phycocyanin pigment in the photodecomposition of the cyanobacterial toxin, microcystin-LR. J. Porphyr. Phthalocyanines 3, 544–551. https://doi.org/10.1002/(sici)1099-1409(199908/10)3:6/7<544::aid-jpp173>3.0.co;2-7.

Sinha, A.K., Eggleton, M.A., Lochmann, R.T., 2018. An environmentally friendly approach for mitigating cyanobacterial bloom and their toxins in hypereutrophic ponds: potentiality of a newly developed granular hydrogen peroxide-based compound. Sci. Total Environ. 637–638, 524–537. https://doi.org/10.1016/j.scitotenv.2018.05.023.

Song, J., Wang, Xuejiang, Ma, J., Wang, Xin, Wang, J., Xia, S., Zhao, J., 2018. Removal of *Microcystis aeruginosa* and Microcystin-LR using a graphitic-C_3N_4/TiO_2 floating photocatalyst under visible light irradiation. Chem. Eng. J. 348, 380–388. https://doi.org/10.1016/j.cej.2018.04.182.

Spoof, L., Catherine, A., 2017. Cyanobacteria samples: preservation, abundance and biovolume measurements. In: Meriluoto, J., Spoof, L., Codd, G. (Eds.), Handbook of Cyanobacterial Monitoring and Cyanotoxin Analysis. John Wiley & Sons, Chichester, UK, pp. 526–537. https://doi.org/10.1002/9781119068761.

Stanier, R.Y., Kunisawa, R., Mandel, M., Cohen-Bazire, G., 1971. Purification and properties of unicellular blue-green algae (order *Chroococcales*). Bacteriol. Rev. 35, 171–205. https://doi.org/10.1128/mmbr.35.2.171-205.1971.

Stirbet, A., Lazár, D., Papageorgiou, G.C., Govindjee, 2018. Chlorophyll *a* Fluorescence in Cyanobacteria: Relation to Photosynthesis. Cyanobacteria: From Basic Science to Applications. https://doi.org/10.1016/B978-0-12-814667-5.00005-2.

Summerfelt, S.T., 2003. Ozonation and UV irradiation - an introduction and examples of current applications. Aquacult. Eng. 28, 21–36. https://doi.org/10.1016/S0144-8609(02)00069-9.

Tao, Y., Hou, D., Zhou, T., Cao, H., Zhang, W., Wang, X., 2018. UV-C suppression on hazardous metabolites in *Microcystis aeruginosa*: unsynchronized production of microcystins and odorous compounds at population and single-cell level. J. Hazard Mater. 359, 281–289. https://doi.org/10.1016/j.jhazmat.2018.07.052.

Triantis, T.M., Fotiou, T., Kaloudis, T., Kontos, A.G., Falaras, P., Dionysiou, D.D., Pelaez, M., Hiskia, A., 2012. Photocatalytic degradation and mineralization of microcystin-LR under UV-A, solar and visible light using nanostructured nitrogen doped TiO_2. J. Hazard Mater. 211–212, 196–202. https://doi.org/10.1016/j.jhazmat.2011.11.042.

Vilela, W.F.D., Minillo, A., Rocha, O., Vieira, E.M., Azevedo, E.B., 2012. Degradation of [D-Leu]-Microcystin-LR by solar heterogeneous photocatalysis (TiO_2). Sol. Energy 86, 2746–2752. https://doi.org/10.1016/j.solener.2012.06.012.

Wang, Xin, Wang, Xuejiang, Zhao, J., Song, J., Su, C., Wang, Z., 2018. Surface modified TiO_2 floating photocatalyst with PDDA for efficient adsorption and photocatalytic inactivation of *Microcystis aeruginosa*. Water Res. 131, 320–333. https://doi.org/10.1016/j.watres.2017.12.062.

Wang, Xin, Wang, Xuejiang, Zhao, J., Song, J., Wang, J., Ma, R., Ma, J., 2017. Solar light-driven photocatalytic destruction of cyanobacteria by F-Ce-TiO_2/expanded perlite floating composites. Chem. Eng. J. 320, 253–263. https://doi.org/10.1016/j.cej.2017.03.062.

Wilson, A.E., Wilson, W.A., Hay, M.E., 2006. Intraspecific variation in growth and morphology of the bloom-forming cyanobacterium *Microcystis aeruginosa*. Appl. Environ. Microbiol. 72, 7386–7389. https://doi.org/10.1128/AEM.00834-06.

Yang, W., Tang, Z., Zhou, F., Zhang, W., Song, L., 2013. Toxicity studies of tetracycline on *Microcystis aeruginosa* and *Selenastrum capricornutum*. Environ. Toxicol. Pharmacol. 35, 320–324. https://doi.org/10.1016/j.etap.2013.01.006.

Yang, Z., Kong, F., Shi, X., Yu, Y., Zhang, M., 2015. Effects of UV-B radiation on microcystin production of a toxic strain of *Microcystis aeruginosa* and its competitiveness against a non-toxic strain. J. Hazard Mater. 283, 447–453. https://doi.org/10.1016/j.jhazmat.2014.09.053.

Zhao, C., Pelaez, M., Dionysiou, D.D., Pillai, S.C., Byrne, J.A., O'Shea, K.E., 2014. UV and visible light activated TiO_2 photocatalysis of 6-hydroxymethyl uracil, a model compound for the potent cyanotoxin cylindrospermopsin. Catal. Today 224, 70–76. https://doi.org/10.1016/j.cattod.2013.09.042.

Zilliges, Y., Kehr, J.C., Meissner, S., Ishida, K., Mikkat, S., Hagemann, M., Kaplan, A., Börner, T., Dittmann, E., 2011. The cyanobacterial hepatotoxin microcystin binds to proteins and increases the fitness of *Microcystis* under oxidative stress conditions. PloS One 6. https://doi.org/10.1371/journal.pone.0017615.